

Optical properties of crystalline tungsten

J. H. Weaver*

Physical Sciences Laboratory, University of Wisconsin, Stoughton, Wisconsin 53589

C. G. Olson and D. W. Lynch

Ames Laboratory-ERDA and Department of Physics, Iowa State University, Ames, Iowa 50010

(Received 12 February 1975)

The optical properties of W are presented between 0.15 and 33 eV. The optical absorptivity or reflectivity was measured at near-normal incidence, and the data were Kramers-Kronig analyzed to determine the dielectric functions. Drude parameters were determined at low energy and were used to separate interband and intraband contributions to ϵ_2 . Structures in ϵ_2 were apparent at 0.42, 0.97, 1.82, 2.35, 3.42, 5.25, 8.8, 11.3, 16.5, 22.5, and 31.5 eV. These features were discussed in terms of recent calculations of Christensen and Feuerbacher and by analogy to other transition metals studied. The loss functions were shown to have three volume plasmons (25.3, 15.2, and 10.0 eV) and three surface plasmons (20.8, 14.8, and 9.7 eV). Structure near 31.5 eV was interpreted as due to N_{VII} core transitions.

INTRODUCTION

In this paper, we report optical measurements of the absorptivity or the reflectivity ($A = 1 - R$ where R is the reflectivity) of crystalline W in the photon energy range 0.15–33 eV. This study can be viewed as a continuation of our efforts to understand the electronic properties of the transition metals, the techniques being the same as those used to investigate hcp Ti,¹ Zr,¹ and Hf,¹ and bcc V,² Nb,³ Ta,² and Mo.² The optical data are presented and compared with existing data, the dielectric functions determined through a Kramers-Kronig analysis of the reflectivity, and the loss functions calculated from ϵ_1 and ϵ_2 ($\epsilon = \epsilon_1 + i\epsilon_2$). Interpretation of features in the dielectric functions is based to a large extent upon recent band calculations of Christensen and Feuerbacher.⁴ Comparisons are made to the other metals when possible, with particular reference to Mo.

Tungsten has been extensively studied by surface-sensitive techniques since it serves as a receptive host for adsorbates and can be cleaned at the atomic level by thermal desorption. Surface properties will not be considered here, however, since our primary interest lies in the bulk properties of W. Comparisons to bulk photoemission results will be made in the course of the discussion.

The electronic bands of W have been calculated by Loucks,⁵ Mattheiss,⁶ and Petroff and Viswanathan.⁷ These have shown that in the absence of relativistic effects, W and Mo have nearly identical Fermi surfaces, but that relativistic effects, particularly spin-orbit effects, are very important in adequately determining the energy levels. The recent calculations by Christensen and Feuerbacher⁴ have included relativistic effects and, like the others, used an augmented-plane-wave technique (APW) to determine $E(\vec{k})$ throughout the Brillouin

zone. The calculations have extended to higher energy than in previous studies,⁸ and, in addition, considered the total and the band-to-band or partial joint density of states (JDOS). Finally, they calculated the interband ϵ_2 under the assumption that matrix elements were constant. This last assumption is tenuous as was shown by Petroff and Viswanathan, but it serves as a first approximation.

The optical properties of W have been investigated by ellipsometric techniques by Nomerovanyaya *et al.*⁹ [electropolished (100) and (110) faces between 0.06 and 4.9 eV], Carroll and Melmed¹⁰ [heat-cleaned in ultrahigh vacuum, (011) face between 1.9 and 3.18 eV], Thurm,^{10a} and Smith.^{10b} Roberts¹¹ studied heat-treated polycrystalline W in the near infrared and visible. Juenker and co-workers¹² also studied heat-cleaned W [~ 2 – ~ 24 eV using discharge-line sources in the vacuum ultraviolet, (011) face]. Only Juenker *et al.* and Udoyev *et al.*¹³ (reflectivity measurements from 1 to 12 eV) reported dielectric functions above ~ 5 eV, although Cox *et al.*¹⁴ measured the reflectivity of vacuum-evaporated W films between 6.2 and 41 eV. Between 25 and 600 eV, the absorption coefficient was determined by Haensel *et al.*¹⁵ The qualitative agreement is quite good for these various studies.

EXPERIMENTAL TECHNIQUES

An electron-beam-melted button of W was obtained within the Ames Laboratory USAEC. Samples were spark-cut from the button and macroetched to reveal large, but unoriented crystal grains (≈ 3 mm). The samples were polished with alumina abrasive to obtain specular surfaces, then electropolished to remove the work-damaged layers. Two electropolishing solutions were used¹⁶ without detectable differences. In all cases the samples were smooth and without ripples or

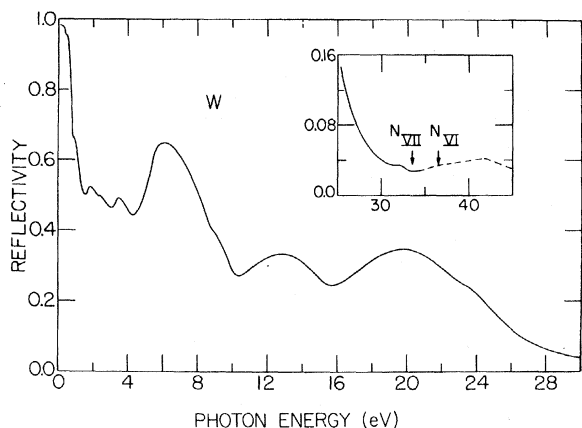


FIG. 1. Reflectivity spectrum of W. The high-energy region is shown in the insert.

small pits.

Immediately prior to loading the sample in the experimental chamber, it was electropolished and dried in a jet of He gas. For the low-energy measurements, the sample was exposed to air for 3–5 min, as it was attached to the sample holder. The holder was then placed in the N_2 -purged chamber, and the chamber was evacuated. For the vacuum ultraviolet (vuv) measurements, the sample was in place within 3 min with roughing pumps started, and within 4 min the chamber pressure was $\sim 5 \times 10^{-3}$ Torr.

A calorimetric technique was used to measure the absorptivity at near-normal incidence between 0.15 and 4.4 eV.¹⁷ Monochromatic radiation was directed upon the sample and absorbed either by it or by a Au-black-coated Cu absorber. Since both elements had small thermal masses and were at 4.2 K, both had measurable temperature increases. By reproducing the temperature excursions with Joule heating, it was possible to determine the power absorbed by each and hence the absorptivity. The reproducibility of the measurements was better than 1% of the value of A at 1 eV, but fell to about 10% of A at 0.15 eV (where A was 0.0178).

Between 4 and 33 eV, the reflectivity¹⁸ was measured at 300 K using the continuum synchrotron radiation from the 240-MeV electron storage ring¹⁹ operated by the Synchrotron Radiation Center (Physical Sciences Laboratory, University of Wisconsin). The beam was incident upon the sample at 10° with the plane of reflection being parallel to the electron orbital plane (the radiation was then 88% p polarized). Since the beam size was ≈ 1 mm in diameter, a single unoriented crystallite was illuminated. It is estimated that the vuv measurements are accurate to (5–7)% of R . Details

of the two techniques have been presented elsewhere.^{17,18}

RESULTS

The reflectivity spectrum of W is shown in Fig. 1. The high-energy region is expanded for clarity and shown in the insert. To show the low-energy region more clearly, the absorptivity ($A = 1 - R$) is shown in Fig. 2. Low-energy interband structure is apparent with the first maximum in A appearing near 0.43 eV. Additional maxima are visible from Fig. 2 at 0.87, 1.57, ≈ 2.25 , 3.06, and 4.3 eV. The maximum in R or the deep minimum in A near 6.1 eV is a characteristic of the bcc transition metals. At higher energy, R has a shoulder visible at about 9.2 eV followed by the minimum at 10.35 eV. Two broad structures are evident at higher energy with maxima at 13 and 19.8 eV and a shoulder at about 23.6 eV. Near 32.1 eV a small feature is evident as shown in the insert of Fig. 1. The dashed line above 33 eV represents the high-energy extrapolation and is based upon the absorption coefficient data of Haensel *et al.*¹⁵

The dielectric functions were determined through a Kramers-Kronig analysis of the reflectivity. To perform the analysis, a high-energy extrapolation made up of the results of Haensel *et al.* to 600 eV (where $R \approx 5 \times 10^{-6}$) followed by a smooth extrapolation to 1000 eV ($R = 1.5 \times 10^{-6}$) was used. In the infrared beyond 0.15 eV, a Drude behavior was assumed with parameters obtained by fitting the absorptivity data to the Drude model. The fit was obtained with $\sigma_0 = 1250 \times 10^{14}$ esu for the static conductivity and $\tau/\hbar = 23.92$ eV⁻¹ for the electronic relaxation time. While no physical meaning should be assigned to these parameters, they were useful in separating intraband and interband contributions to the total ϵ_2 .

The interband ϵ_2 is shown in Fig. 2. A sharp onset is observed with a maximum at 0.42 eV. Additional maxima are evident at 0.97, 1.82, 2.35, 3.42, and 5.25 eV. The higher-energy features

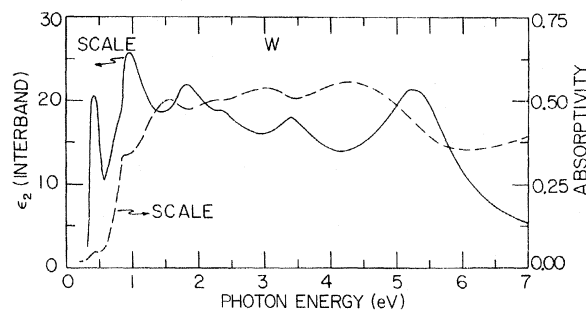


FIG. 2. Absorptivity ($A = 1 - R$) of W below 7 eV (right-hand scale). The interband ϵ_2 is also shown (left-hand scale).

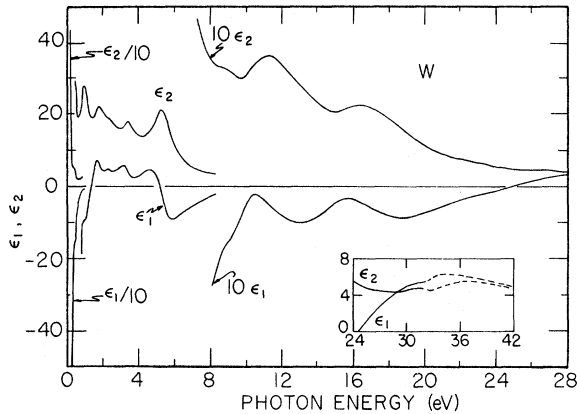


FIG. 3. Real and imaginary parts of the dielectric function of W. The high-energy region is shown in the insert.

are shown in Fig. 3 together with the real part of the dielectric function, ϵ_1 . The shoulder in ϵ_2 at 8.8 eV corresponds to the shoulder in R at 9.2 eV. ϵ_2 then goes through a minimum at 9.8 eV with subsequent features at 11.3, 16.5, ≈ 22.5 , and 31.5 eV. ϵ_1 rises sharply at low energy with features at about 0.4 and 0.9 eV and maxima at 1.68, 2.25, 3.15, 4.6, ≈ 8.5 (shoulder), 10.5, 15.8, ≈ 22.5 (shoulder), and 30 eV. Zero crossings occur at 1.3, 5.2, and 23.8 eV.

DISCUSSION

The low-energy optical properties of W are influenced to a large extent by the magnitude of relativistic effects, particularly spin-orbit splitting of the bands along the $\langle 100 \rangle$ directions of the zone. This can be seen graphically by comparing ϵ_2 for W with ϵ_2 for Mo,² since, in the absence of relativistic effects, the two have nearly identical Fermi surfaces.^{5,6} In Mo, a single, rather broad structure in the static ϵ_2 was apparent with a maximum at 1.80 eV.² In W, structures are apparent at 0.42 and 0.97 eV which have no counterparts in the Mo spectrum. The structures at higher energy do find analogous features in Mo.

It was shown in Figs. 1-3 that the first interband maximum is at 0.42 eV. To interpret the structure, one can compare with the bands of Christensen and Feuerbacher⁴ (Fig. 4) and with the calculated band-to-band JDOS. These show that direct transitions have a threshold at about 0.35 eV, corresponding to the spin-orbit gap formed between bands 4 and 5 along $\Gamma(\Delta)H$. The experimental feature at 0.97 eV can also be related to transitions between 3 and 4, and 4 and 5 along the same direction.⁴

A thermoreflectance experiment showed that the first structure in Mo was actually a double feature.²⁰ The origin of the structure was identified to be along the $\langle 100 \rangle$ directions with the initial states being the nearly degenerate parallel third

and fourth bands and the final states being the fifth band. The measurements showed the separation of bands 3 and 4 to be approximately 0.24 eV at E_F . In W, the splitting should be considerably larger, but one should not expect optical transitions between the two formerly degenerate bands. No structure is observed in the experimental ϵ_2 although Christensen and Feuerbacher estimated the threshold to be approximately 0.5 eV. Instead, two maxima are observed in ϵ_2 at 1.82 and 2.35 eV, and it seems reasonable to give as their origin transitions like 3 \rightarrow 5 and 4 \rightarrow 5 along $\Gamma(\Delta)H$.

It should be stressed that for metals large volumes of k space contribute to optical absorption. The influence of critical points is much reduced from what is observed in semiconductors and insulators. While identifications are made with respect to a direction or symmetry line of k space, it should be realized that large volumes of k space might be involved.

The structure at 3.42 eV in W finds a counterpart in Mo at 2.35 eV. On the basis of the temperature dependence of the structure in Mo,²⁰ we argued that the structure probably did not involve transitions to or from E_F . The third, fourth, and fifth bands along Σ are probably responsible for the structure. The initial states in the third band have $\approx 50\%$ s - and p -like character while the final states are almost purely d -like.²¹

Structure appears in W at 5.25 eV which is difficult to unambiguously relate to parts of the zone. The bands along F , G , Σ , and Λ could all be contributing. The analogous peak in Mo lies at 4.1 eV.

The feature in W at 8.8 eV, and in Mo at 7.1 eV, can probably be related to transitions from the first to the fourth band at E_F along Σ and Λ . Harmon has shown the initial-state wave functions to

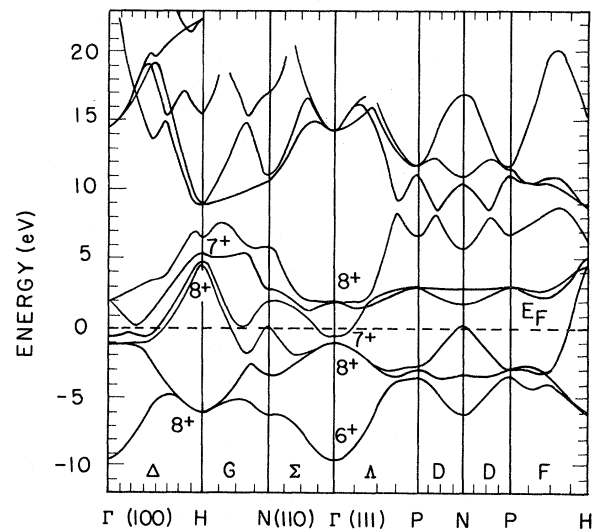


FIG. 4. Electron energy bands calculated by Christensen and Feuerbacher (Ref. 4).

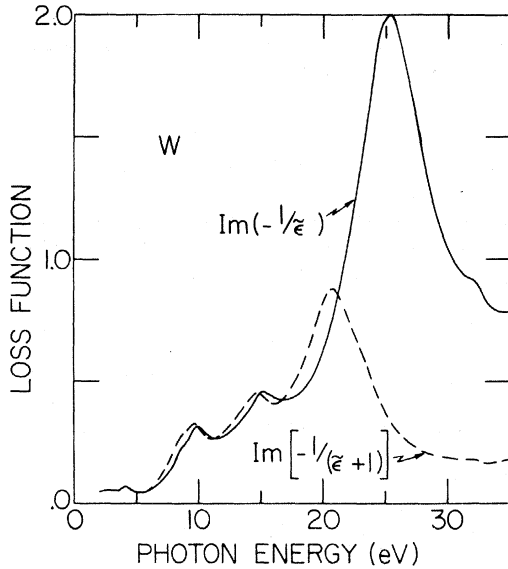


FIG. 5. Electron-energy-loss functions: $\text{Im}(-1/\bar{\epsilon})$ is the volume-loss function and $\text{Im}[-1/(\bar{\epsilon}+1)]$ is the surface-loss function.

be $\approx 90\%$ p -like and $\approx 10\%$ s -like and the final-state wave functions to be $\approx 90\%$ d -like.²¹

It would be tempting to compare the experimental feature at 8.8 eV with theoretical structure near 9 eV (Ref. 4). The calculated feature involves $N2 \rightarrow N6$ transitions; but as was pointed out by Koelling *et al.*,²² only transitions to the fourth band at N are allowed by electric-dipole selection rules ($N4$ has symmetry N_5^+ ; the other states have symmetry N_5^+). Further, for Mo, the counterpart would appear at roughly²³ 7.8 eV instead of the measured 7.1 eV. Harmon's calculations show the second and sixth bands at N to have almost completely d -like character.

Angularly resolved photoemission measurements⁴ have recently shown the $\langle 100 \rangle$ directions to have direct optical transitions originating in the first and second bands near H with final states just above the work function threshold (4.3 eV) and continuing along the sixth band toward H. The initial state character is nearly pure d -like while the final states have mixed p -like ($\approx 75\%$) and f -like ($\approx 15\%$) character. These transitions, doubtless, contribute to the optical absorption between 9 and 13 eV, but cannot be the sole source of the high-energy structure seen in Fig. 4. Such high-energy absorption is characteristic of the $4d$ and $5d$ transition metals,^{1-3,24} and is thought to arise from states within the d bands, the final states lying well above E_F and having largely s -, p -, and f -like character. Recent calculations for Pd tend to support this,²⁵ but further calculations, probably including matrix elements, are needed.

At the highest energies, we have observed a structure which can be related to the N_{VI} core

levels. The broad maximum in ϵ_2 is centered at 31.5 eV. Recent x-ray photoemission data²⁶ have shown the N_{VII} and N_{VI} levels to lie at 31.7 ± 0.1 and 33.9 ± 0.1 eV, respectively. These are displaced somewhat from the values quoted by Bearden and Burr²⁷ (33.6 ± 0.4 and 36.5 ± 0.4 eV, respectively). The arrows in Fig. 1 reflect the Bearden and Burr energies.

The probability that a surface or volume plasmon will be excited is given by the respective loss function, $\text{Im}[-1/(\bar{\epsilon}+1)]$ and $\text{Im}(-1/\bar{\epsilon})$. These functions have been determined from our dielectric functions and are shown in Fig. 5. The dominant structure in the volume-loss function is a maximum at 25.3 eV and can be compared to the calculated free-electron plasmon energy of 22.82 eV. Since there is considerable interband activity near 25 eV, it is not surprising that the energy is shifted from the free-electron value. More dramatically shifted, however, is the surface plasmon which one might expect to occur at roughly $22.82/\sqrt{2} = 16.1$ eV. The surface plasmon actually appears at 20.8 eV. Similar large deviations from the simple free-electron theory have been observed in the other transition metals.^{1-3,24}

Two additional pairs of structures appear in the loss functions which can also be identified as volume and surface plasmons with energies of 10.0 and 9.7 eV, respectively, for one pair, and 15.2 and 14.8 eV for the other. Like the other metals studied,¹⁻³ W has a volume plasmon close to where the reflectivity drops dramatically (~ 10 eV) and ϵ_1 predictably approaches zero with positive slope. Since the slope of ϵ_1 is steep, the corresponding surface plasmon lies close in energy to the volume plasmon. The peak near 15.2 eV is associated with similar features in ϵ_1 and ϵ_2 . It is more prominent in W than in Nb, Mo, and Ta, for which the corresponding peaks were not identified as plasmas. In view of the W loss functions, it is felt that each of these bcc transition metals has three volume and three surface plasmons.

Electron-energy-loss measurements have shown the existence of structures in good agreement with our loss-function maxima.²⁸ Since most measurements have been in electron reflection, there has been little chance of separating volume from surface effects, and the corresponding structures near 10 eV are probably a combination of the two plasmons. Optical dielectric functions allow the separation to be made.

Larger figures and tables can be obtained from the authors.

ACKNOWLEDGMENTS

The authors are grateful to F. A. Schmidt of the Ames Laboratory for providing the W button, H. H. Baker for advice in sample preparation, and Pro-

fessor L. Thomas for sending us a copy of Ref. 10(a). The support of the Synchrotron Radiation Center staff, particularly E. M. Rowe, R. A. Otte,

and C. H. Pruett is appreciated. The Synchrotron Radiation Center is presently supported under NSF Grant No. DMR-7415089.

- *Supported in part under Air Force Office of Scientific Research Contract No. F44620-70-C-0029 and in part by the National Science Foundation under Grant No. DMR-7415089.
- ¹D. W. Lynch, C. G. Olson, and J. H. Weaver, *Phys. Rev. B* **11**, 3617 (1975).
- ²J. H. Weaver, D. W. Lynch, and C. G. Olson, *Phys. Rev. B* **10**, 501 (1974).
- ³J. H. Weaver, D. W. Lynch, and C. G. Olson, *Phys. Rev. B* **7**, 4311 (1973).
- ⁴N. E. Christensen and B. Feuerbacher, *Phys. Rev. B* **10**, 2349 (1974).
- ⁵T. L. Loucks, *Phys. Rev.* **139**, A1181 (1965); **143**, 506 (1966).
- ⁶L. F. Mattheiss, *Phys. Rev.* **139**, A1893 (1965).
- ⁷I. Petroff and C. R. Viswanathan, *Phys. Rev. B* **4**, 799 (1971).
- ⁸The calculations of Ref. 7 extended to ≈ 16 eV above E_F , but they did not include relativistic effects in their calculations.
- ⁹L. V. Nomerovannaya, M. M. Kirillova, and M. M. Noskov, *Zh. Eksp. Teor. Fiz.* **60**, 748 (1971) [*Sov. Phys. JETP*, **33**(2), 405 (1971)] *Fiz. Tverd. Tela* **14**, 633 (1972) [*Sov. Phys.—Solid State* **14**, 541 (1972)].
- ¹⁰J. J. Carroll and A. J. Melmed, *J. Opt. Soc. Am.* **61**, 1470 (1971); (a) S. Thurm, thesis (Technische Universität Berlin, 1974) (unpublished); (b) T. Smith, *J. Opt. Soc. Am.* **62**, 774 (1972).
- ¹¹S. Roberts, *Phys. Rev.* **114**, 104 (1959).
- ¹²D. W. Juenker, L. J. LeBlanc, and C. R. Martin, *J. Opt. Soc. Am.* **58**, 164 (1968); and L. J. LeBlanc, J. S. Farrell and D. W. Juenker, *ibid.* **54**, 456 (1964).
- ¹³Yu. P. Udoyev, N. S. Koz'yakova, and M. L. Kapitza, *Fiz. Met. Metalloved.* **31**, 439 (1971). *Phys. Met. Metallogr.* **31**(2), 229 (1971).
- ¹⁴J. T. Cox, G. Hass, J. B. Ramsey, and W. R. Hunter, *J. Opt. Soc. Am.* **62**, 781 (1972).
- ¹⁵R. Haensel, K. Radler, B. Sonntag, and C. Kunz, *Solid State Commun.* **7**, 1495 (1969).
- ¹⁶6% perchloric acid by volume in methanol cooled to ≈ 200 K by a solution of dry ice and acetone; and 175-ml H_2O , 25-ml H_2O_2 (30% solution) and 4 g of NaOH at 300 K, not agitated.
- ¹⁷L. W. Bos and D. W. Lynch, *Phys. Rev. B* **2**, 4784 (1970).
- ¹⁸C. G. Olson and D. W. Lynch, *Phys. Rev. B* **9**, 3159 (1974).
- ¹⁹E. M. Rowe and F. E. Mills, *Part. Accel.* **4**, 211 (1973).
- ²⁰J. H. Weaver, C. G. Olson, D. W. Lynch, and M. Piacentini, *Solid State Commun.* **16**, 163 (1975).
- ²¹B. Harmon (private communication).
- ²²D. D. Koelling, F. M. Mueller, and B. W. Veal, *Phys. Rev. B* **10**, 1280 (1974).
- ²³See the band calculations of the N. E. Christensen, in *Computational Solid State Physics*, edited by F. Herman, N. W. Dalton, and T. Koehler (Plenum, 1970), p. 155; and Report No. 95, Technical University of Denmark (unpublished). See also the bands of Ref. 22.
- ²⁴J. H. Weaver, *Phys. Rev. B* **11**, 1416 (1975).
- ²⁵O. K. Andersen and O. Jepsen have calculated the high-lying bands of Pd including *s*- and *p*-like states. N. E. Christensen has used those bands to determine the JDOS and band-to-band JDOS.
- ²⁶C. M. Penchina, E. Sapp, J. Tejada, and N. Shevchik, *Phys. Rev. B* **10**, 4187 (1974).
- ²⁷J. A. Bearden and A. F. Burr, *Rev. Mod. Phys.* **39**, 125 (1967).
- ²⁸G. A. Harrower, *Phys. Rev.* **102**, 340 (1956); D. Edwards and F. M. Prost, *J. Chem. Phys.* **55**, 5175 (1971); C. J. Powell, J. L. Robins, and J. E. Swan, *Phys. Rev.* **110**, 657 (1958); E. J. Scheibner and L. N. Thorp, *Surface Sci.* **8**, 247 (1967). See also Ref. 26.